patients with glioma. *Cancer* 1988;62:1074–1078.

8. Yonekura Yoshihisa ABE, Benua RS, Brill AB, et al. Increased accumulation of 2-deoxy-2[^{18}F]fluoro-D-glucose in liver metastases from colon cancer. *J Nucl Med* 1982;23:1133–1137.

9. Fukuda H, Matsuzawa T, Abe Y, et al. Experimental study for cancer diagnosis with positron labeled fluorinated fluose analogs: [^{18}F]-2-fluoro-2-deoxy-D-mannose: a new tracer for cancer detection. *Eur J Nucl Med* 1982;7:294–297.

10. Phelps ME, Huang SC, Hoffman EJ, Selin C, Sokoloff L, Kuhl DE. Tomographic measurements of local cerebral glucose metabolic rate in humans with [^{18}F]2-fluoro-2-deoxy-D-glucose: validation of method. *Ann Neurol* 1979;6:371–388.

11. Monakhov NK, Neistadt EL, Shaviovlkii MM, Shvartsman AL, Neifakh SA. Physicochemical properties and isoenzyme composition of hexokinase from normal and malignant human tissues. *J Natl Cancer Inst* 1978;61:27–34.

12. Bustamante E, Morris HP, Pedersen PL. Energy metabolism of tumor cells. *J Biol Chem* 1981;256:8699–8704.

13. Knox WE, Jamdar SC, Davis PA. Hexokinase, differentiation and growth rate of transplanted rat tumors. *Cancer Res* 1970;30:2240–2244.

14. Weinhouse S. Glycolysis, respiration, and enzyme deletions in slow-growing hepatic tumors. *Gann Monogr* 1966;1:99–115.

15. Sokoloff L, Reivich M, Kennedy C, et al. The [^{14}C]deoxyglucose method for the measurement of local cerebral glucose utilization: theory, procedure, and normal values in the conscious and anesthetized albino rat. *J Neurochem* 1977;28:897–916.

16. Breedis C, Young G. The blood supply of neoplasms in the liver. *Am J Pathol* 1954;30:969–985.

17. Herholz K, Ziffling P, Staffen W, et al. Uncoupling of hexose transport and phosphorylation in human gliomas demonstrated by PET. *Eur J Cancer Clin Oncol* 1988;24:1139–1150.

18. Criss WE. A review of isoenzymes in cancer. *Cancer Res* 1971;31:1523–1542.

19. Weber G, Lui S, Takeda E, Denton JE. Enzymology of human colon tumors. *Life Sci* 1980;27:793–799.

20. Sharma RM, Sharma C, Donnelly AJ, Morris HP, Weinhouse S. Glucose-ATP phosphotransferases during hepatocarcinogeneses. *Cancer Res* 1965;25:193–199.

21. Weber G, Cantero A. Glucose-6-phosphatase activity in normal, precancerous, and neoplastic tissues. *Cancer Res* 1955;15:105–108.

22. Gallagher BM, Fowler JS, Gutterson NI, MacGregor RR, Wan CN, Wolf AP. Metabolic trapping as a principle of radiopharmaceutical design: some factors responsible for the biodistribution of [^{18}F]2-deoxy-2-fluoro-D-glucose. *J Nucl Med* 1978;19:1154–1161.

23. Patlak C, Blasberg RG, Fenstermacher JD. Graphical evaluation of blood-to-brain transfer constants from multiple uptake data. *J Cereb Blood Flow Metab* 1983;3:1–7.

24. Strauss LG, Clorius JH, Schlag P, et al. Recurrence of colorectal tumors: PET evaluation. *Radiology* 1989;170:329–332.

25. Weber G, Morris HP, Love WC, Ashmore J. Comparative biochemistry of hepatomas. II. Isotope studies of carbohydrate metabolism in Morris hepatoma 5123. *Cancer Res* 1961;21:1406–1411.

EDITORIAL
Quantitating Tumor Glucose Metabolism with FDG and PET

The glucose analog 2-[^{18}F]fluoro-2-deoxy-D-glucose (FDG) was first utilized with positron emission tomography (PET) in humans to quantify cerebral glucose metabolism (1–3), based on a tracer kinetic method initially developed for autoradiographic rat studies with ^{14}C-deoxyglucose by Sokoloff et al. (4). The method has been extended, with appropriate modifications, to other organ systems, including the heart (5). Because of the high glycolytic rate of many malignancies, qualitative and quantitative PET FDG imaging evaluations of tumors of the central nervous system (CNS) and other organ systems have demonstrated the potential utility of the method to detect the presence of malignant tissue and to quantify changes in tumor glycolysis during and after treatment (6). While reported quantitative PET FDG tumor studies during and after treatment are limited in number, most of these investigations have concerned

radiotherapy, although some results with chemotherapy have also been reported (7–12). The majority of quantitative PET FDG tumor studies, other than those of astrocytomas (13, 14), have been based on nonkinetic evaluations of relative tumor FDG uptake, compared either to normal tissue or to injected dose per body weight (6,7,15).

Following facilitated diffusion from plasma to tissue, FDG is phosphorylated by hexokinase and trapped intracellularly as FDG-6-PO$_4$ (2,4,16,17), with, for most tissues, a very slow rate of dephosphorylation. Therefore, the 511 keV photons resulting from annihilation of the positron emitted by ^{18}F originate both from FDG distributed between plasma and tissue, and from FDG-6-PO$_4$ within cells. After about 40 min following intravenous injection of FDG, the majority of the ^{18}F label in the brain, heart, and most tumors originates from intracellular FDG-6-PO$_4$. In tissues with low rates of glucose-6-phosphatase mediated dephosphorylation, the accumulated amount of FDG-6-PO$_4$ is proportional to the glycolytic rate. Since by 40 min the majority of tissue activity

is in the form of FDG-6-PO$_4$, images of total ^{18}F activity represent relative rates of glycolysis. This approximation is appropriate over a wide range of glycolytic rates, although it is less accurate at very low glycolytic rates.

One may therefore analyze PET FDG tumor studies on three levels: (1) qualitative inspection of static images, taken 40 min after injection, for identification of high local activities characteristic of aggressive tumors; (2) nonkinetic quantitative analyses of relative lesion activity concentration compared to injected dose per body weight or region of interest ratio methods; and (3) kinetic evaluations of tumor glucose metabolic characteristics, utilizing either the closed-form solution for the FDG model (Equation 2 below) and a priori estimates of model parameters (i.e., rate constants) with images obtained at a single time (the autoradiographic method) or employing a dynamic acquisition sequence and directly estimating model rate constants with nonlinear regression (Equation 1 below) (MR, in units of μmol/100 g/min) (2–4).

The kinetic methods then produce estimates of the tissue glucose meta-

bolic rates with either of the following equations:

$$MR = \frac{C_p}{LC} \frac{K_1^* k_3^*}{(k_2^* + k_3^*)}$$

$$= \frac{C_p}{LC} K, \quad \text{Eq. 1}$$

where $K = \frac{K_1^* k_3^*}{(k_2^* + k_3^*)}$

or, the autoradiographic method:

$$MR =$$

$$\frac{C_p\left[C_i^*(T) - \frac{K_1^*}{\alpha_2 - \alpha_1}\{(k_3^* - \alpha_1)e^{-\alpha_1 t} + (\alpha_2 - k_3^*)e^{-\alpha_2 t}\} \otimes C_p^*(t)\right]}{(LC)\frac{k_2^* + k_3^*}{\alpha_2 - \alpha_1}(e^{-\alpha_1 t} - e^{-\alpha_2 t}) \otimes C_p^*(t)},$$

Eq. 2

where $\otimes$ denotes operation of convolution, and

$$\alpha_1 = (k_2^* + k_3^* + k_4^*$$
$$- \sqrt{(k_2^* + k_3^* + k_4^*)^2 - 4k_2^* k_4^*})/2$$
$$\alpha_1 = (k_2^* + k_3^* + k_4^*$$
$$+ \sqrt{(k_2^* + k_3^* + k_4^*)^2 - 4k_2^* k_4^*})/2.$$

Eq. 3

The rate constants K^*_1 and k^*_2 refer to forward and reverse capillary transport of FDG, while k^*_3 and k^*_4 refer to phosphorylation of FDG and dephosphorylation of FDG-6-PO$_4$, respectively. C_p is the plasma-glucose concentration, $C^*_i(T)$ is the tissue concentration of FDG + FDG-6-PO$_4$ at time of imaging (T), $C^*_p(t)$ is the plasma activity concentration as a function of time (the input function), and the lumped constant (LC) is a term derived from the principles of competitive enzyme kinetics that describe the differing transport and phosphorylation characteristics of glucose and FDG (1–4).

Because the autoradiographic method (Equation 2) requires a priori population estimates of the model rate constants and the lumped constant, it is generally not applicable for neoplasms outside of the CNS for which population estimates of these parameters

are not yet available. If one assumes that LC in a given tumor is constant over time, then quantitative estimates of absolute changes in tumor glucose metabolism are possible with Equation 1 when the model rate constants are measured directly with a dynamic imaging sequence.

Enhanced aerobic glycolysis of malignant cells, first noted by Warburg (18,19), facilitates detection and quantification of tumor glucose metabolic rates with the FDG and PET. Advances in the understanding of the molecular biology of cancer also have implications for quantitative biochemical imaging with PET. Flier et al. (20) demonstrated that in cultured rodent fibroblasts transfected with ras or src oncogenes, the uptake of [³H]2-deoxy-D-glucose was significantly increased. The production of the transporter protein for glucose and the mRNA for this protein were also increased. Thus, amplified glucose transport capability may be one of the factors associated with the high glycolytic rate of neoplastic cells, and illustrates that tumor FDG kinetics (i.e., transport and phosphorylation) may differ from normal tissues in a variety of ways.

It is important to remember that the rate constants are not universal constants, but rather constants reflecting a particular steady state condition of transport and phosphorylation. Changes in rates of transport and metabolism occur with changes in the rate constants and precursor pool concentrations. In recognition of this, the original Sokoloff model was formulated to have a low sensitivity to the absolute value of the rate constants themselves. This was possible because the end product of metabolism, deoxyglucose-6-PO$_4$, was stoichiometrically accumulated and retained in tissue over the time of measurement. This permits a great deal of latitude in the use of average or population values for rate constants and in the qualitative interpretation of images. There are, however, limits to this flexibility that must be defined in various tissues and metabolic states.

In this issue of the Journal, Okazumi et al. (21) evaluated the FDG rate constants K^*_1, k^*_2, k^*_3, and k^*_4 in 35 patients with liver tumors (23 with either hepatocellular carcinomas or cholangiocarcinomas, 10 with metastatic disease to the liver, and 2 with liver hemangiomas), in 12 normal volunteers and in 10 patients with cirrhosis of undescribed etiology. Utilizing a 60-min dynamic imaging sequence consisting of 2-min scans for the first 10-min interval and 10-min scans thereafter, they estimated the model rate constants with nonlinear regression methods, focusing their analysis on small regions of interest in areas of peak tumor metabolic activity. They did not include a tissue-blood volume term in their model, and arterial blood samples were used as the input function. Evidently to minimize the partial volume effect, all the tumors evaluated in this series were 3 cm or larger in diameter. Additionally, the authors directly assayed tissue hexokinase levels in resected specimens of hepatocellular carcinoma (seven cases), liver metastases (two cases) and one hemangioma.

While the authors investigated a variety of relationships between the rate constants in the patients in their series, the most important were the significant, if not striking, correlation between k^*_3 and hexokinase activity (r = 0.658) in the above assayed cases, a threshold value for k^*_3 of 0.025 min^{-1}, above which all lesions were malignant, k^*_4 values near zero for cholangiocarcinoma and liver metastases, and k^*_4 values of similar or greater magnitude than k^*_3 for hepatocellular carcinoma, cirrhotic livers and controls. Because, as noted by the authors, the liver contains a high concentration of glucose-6-phosphatase activity, the relatively high values of k^*_4 in tumors of liver cell origin and in normal and cirrhotic liver are not surprising. Interestingly, the variable intensity of net FDG uptake in hepatocellular carcinomas on late images could be explained by variable levels of k^*_4, even when k^*_3 (and hexokinase) values were similar. The authors

proposed using the k^*_4/k^*_3 ratio as an index of differentiation of hepatocellular carcinoma (a higher value is more similar to normal liver tissue, a lower value suggests malignant dedifferentiation). The investigators also describe two cases of hepatocellular carcinoma treated with transcatheter arterial embolization (TAE) who had significant decreases in k^*_3 following intervention.

The work represents an interesting contribution to the PET FDG oncology literature, because so little published FDG kinetic data for non-CNS tumors exist. Okazumi et al. have also demonstrated the potential utility of analyzing FDG model microparameters in hepatic neoplasms, and have shown that metabolic characteristics of specific organ systems must be considered when analyzing FDG kinetics. Their results following transcatheter arterial embolization are interesting, but too limited in numbers of subjects to indicate more than the potential usefulness of FDG assays following interventions.

One omission from the results reported by Okazumi et al. was a description of the subjects' dietary states and measurements of their plasma-glucose levels. Equation 1 indicates that local glucose metabolic rates are a function of K, the plasma-glucose level and the lumped constant. While the lumped constant is not known for normal liver and liver pathological conditions, one may still assess changes in absolute rates of tumor glucose metabolism if (using Equation 1) it is assumed that LC for a given lesion does not change, and if the plasma-glucose concentration is measured. Significant variations in plasma-glucose concentrations could affect the values of the FDG rate constants.

Two of the most important applications of PET FDG studies in oncology promise to be the quantitative characterization of tumor glycolytic characteristics as a way of differentiating subtypes of neoplasms, as demonstrated by Okazumi et al., and, perhaps more importantly, quantitative measurements of tumor glycolytic rates during and after treatment. Maximizing the accuracy and defining the precision of such measurements will be necessary, particularly if numerical results generated by one institution are to have significance for other sites. In oncology, where multicenter trials are often the only means to generate enough data to meaningfully assess clinical trials and treatment regimens, this process will be particularly important.

Factors to be considered in defining and improving the precision of measurements of tumor FDG uptake include:

1. **Patient Preparation.** While the impact of dietary preparation, including duration of fasting, has been evaluated for the heart and brain (5), little information exists concerning the impact of diet on FDG studies in tumors and other tissues. However, as discussed above, it is prudent to evaluate patients in a reproducible dietary state, such as fasting. With mediastinal malignancies, such as lymphomas, fasting will facilitate lesion detection by minimizing myocardial FDG uptake.

2. **Tomograph Characteristics.** This topic has been the subject of reviews (22), but a few critical parameters to consider include in plane and axial resolution, axial field of view (number of rings and slice thickness), and counting sensitivity. Measured attenuation correction methods are mandatory outside of the brain if truly quantitative measurements are to be performed.

A major issue is the use of whole-body PET tomography versus a limited axial range of transaxial, coronal and saggital views. Since metastatic disease is an important factor in therapeutic decisions and prognosis, whole body tomographic studies provide a means, in a single examination, to determine the distribution of organ involvement of disease (23, 24). With FDG, these studies can be performed immediately after completing a quantitative kinetic study.

Because tumors will include a wide range of physical sizes and will change over time, assessing the impact and, when possible, correcting for the partial volume induced errors in tumor radiopharmaceutical concentration measurements is important. Correlation and registration of PET results with anatomic imaging modalities such as MRI and CT will permit direct measurements of tumor recovery coefficients (the fraction of true isotope concentration recovered in a given region of interest). Another approach is to estimate the tumor size (and the recovery coefficient) and radioactive concentration together by assuming a defined shape or configuration of the lesion (25, 26). A third approach is to use PET dynamic imaging itself: object size (and recovery coefficient) can be included as a parameter in a kinetic model for an appropriate physically characterized tomography (27).

3. **Model Formulation and Tumor Metabolic Characteristics.** Nonkinetic measurements of tumor FDG uptake, such as the "standard uptake value" (SUV) and "differential uptake ratio" (DUR) (7,15) that are based on tissue activity levels and body weight are, to a certain extent, model independent. They obviate the need to address issues related to the FDG model per se, including the rate constants, lumped constant, and model configuration, but are time-dependent quantities that are still affected by all factors related to FDG kinetics and quantification. With appropriate validation and attention to reproducibility of the measurement protocol, the nonkinetic measurements have the advantage of technical simplicity. Additionally, if there is little loss of FDG-6-PO_4 from tissue (low values of k^*_4), the total tumor activity level will be proportional to the glycolytic rate. As illustrated by the work of Okazumi et al., however, some tumors may have more complex kinetics that can only be understood with a true kinetic acquistion and analytical approach. It must also be remembered that if k^*_4 is numerically small, considerably more time than a one hour acquisition

sequence is necessary to accurately estimate its value (*13,28*). Of course, if k*₄ is small, it has little effect on the glycolytic estimates at shorter time intervals.

Refinements of the FDG model may, in some tumor systems, be necessary. Addition of a tissue vascular space to the model provides improved estimates of metabolism when the blood activity is a significant fraction of the tissue activity, and in addition, it yields physiological insight into the relative blood volume of tumors, as demonstrated in astrocytomas (*13*). Because the relative vascular volume on non-CNS tumors is probably variable in different tumors, this issue remains to be explored.

Another issue of potential significance to FDG tumor kinetic studies is tissue heterogeneity. While the effect of tissue heterogeneity has been investigated in some detail for PET measurements of cerebral blood flow with ¹⁵O methods (*29,30*), only a few studies of tissue heterogeneity effects with cerebral deoxyglucose studies have been reported (*31,32*). Because some tumors will be markedly heterogeneous, understanding this effect could be important.

4. The Input Function. As discussed by Okazumi et al., the input fraction to the liver actually consists of two inputs: the hepatic arterial and portal venous systems. Approximating this input function with peripherally measured arterial concentrations is reasonable if model parameters are interpreted appropriately. The biphasic arrival of a bolus of activity to the liver permits kinetic estimations of the relative flow through the hepatic arterial and portal venous systems with tracers that are not highly extracted by the liver (*33*). In the context of FDG studies of hepatic neoplasms, it is the glycolytic characteristics of tumors that are of primary interest. Nevertheless, one must exercise appropriate caution interpreting the numerical value of the transport rate constant K*₁ in this context. Model configurations incorporation the concentration gradient across the

capillary have also been developed (*34*) and may have utility in tumor studies.

Additional potential issues of concern relative to the input function include the advisability of approximating arterial concentrations with venous samples or arterialized venous samples, as previously investigated for kinetic studies of the brain (*13*). In some circumstances, the input function may be obtained directly from the images, with a rapid dynamic imaging sequence. While this is most feasible if the heart is in the field of view (*35,36*), modern PET systems are also capable of generating good quality input functions from the abdominal aorta, if partial volume corrections are applied (*26*).

All FDG tumor quantitative methods, including tracer kinetic models, must strike a balance between being comprehensive, but impractical, and

very simple, but potentially misleading. The autoradiograpic FDG method has the advantage of yielding absolute estimates of glucose metabolism, but requires a priori estimates of representative population rate constants, a numerical value of the LC, and an understanding of the physiological state of tissue. These conditions are not met for oncology studies at this time. Kinetic studies with nonlinear regression, like those performed by Okazumi, yield potentially useful numerical information, but are somewhat cumbersome computationally and are fairly labor-intensive in terms of regions of interest definition.

A potentially useful alternative is parametric imaging of relevant physiological and biochemical parameters. For tissues with low or defined values of k*₄, the Patlak graphical approach yields pixel by pixel estimates of K that are directly proportional to tissue
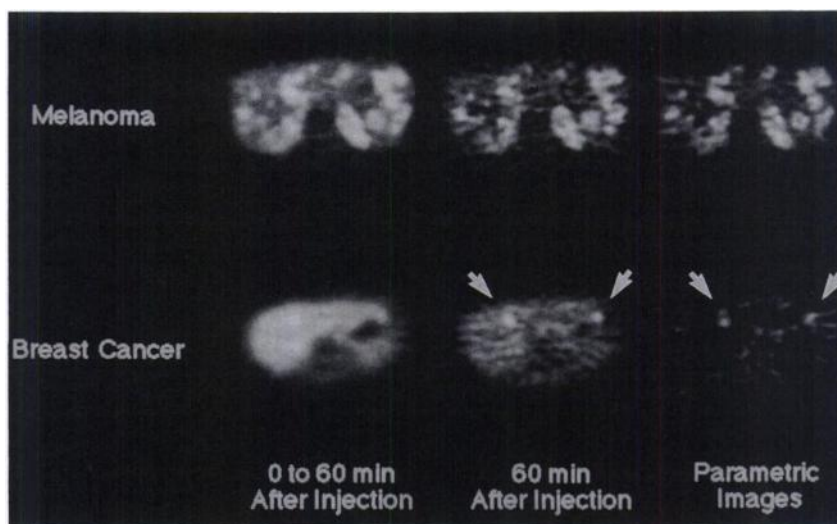

FIGURE 1 Representative transaxial FDG images from two patients with metastatic disease to the liver. The row of images above is from a patient with metastatic melanoma, and the images below are from a patient with metastatic breast cancer. Images on the left represent summed images from time of injection to 60 minutes after injection, images in the center are a single image at 60 minutes after injection, and images on the right are parametric images, scaled in units of the composite parameter K (for net uptake and phosphorylation of FDG, Equation 1) that is proportional to the glucose metabolic rate. Both patients had multiple hepatic metastases that are better defined on single frame image (center) than on the summed images (left). The melanoma patient had many metastases in the liver and spleen, while the breast cancer patient had several metastases, two of which are identified by arrows on the single frame and parametric images. The parametric images on the right illustrate better lesion contrast than the summed or single time images, because the method tends to minimize the image contribution of structures not progressively incorporating FDG, such as vascular structures and, in this case, normal liver because of its high glucose-6-phosphatase activity. The method can be appropriately modified to incorporate the effects of non-zero values of k*₄ (35, 37, 38).

glucose metabolism (Equation 1). Choi et al. (35) have demonstrated the utility of this method in quantifying myocardial glucose metabolism.

Figure 1 illustrates this method applied to two patients with metastatic disease to the liver. The method (39) does not require nonlinear regression and is therefore computationally fast. It increases the contrast of tissues, such as tumors, with high glycolytic rates, relative to surrounding tissues, with lower metabolic rates, high local tissue vascular content, or other factors that result in a lower fraction of irreversibly bound FDG-6-PO$_4$ in tissue, including, in the case of normal liver, the high levels of glucose-6-phosphatase activity. Herholz (40) has also demonstrated the feasibility of parametric imaging of FDG parameters with pixel by pixel nonlinear regression, with appropriate filtering of data, to reduce noise, prior to fitting.

PET FDG studies of neoplasms produce both images of relative FDG uptake and, with appropriate processing, numerical estimates of tumor rate constants for capillary transport, phosphorylation, dephosphorylation and other parameters. Most fundamentally, these studies produce qualitative and quantitative evaluations of tumor glycolytic rates, and will improve our understanding of the most appropriate and reliable methods to employ PET for evaluating the accelerated glycolytic rates associated with malignant transformation. The potential implications for oncological applications of these numerical results are just now beginning to become apparent.

Randall A. Hawkins
Yong Choi,
Sung-Cheng Huang,
Cristina Messa,
Carl K. Hoh,
Michael E. Phelps
UCLA School of Medicine
Los Angeles, California

REFERENCES

1. Reivich M, Kuhl DE, Wolf A, et al. The (^{18}F)-fluorodeoxyglucose method for the measurement of local cerebral glucose utilization in man. Cir Res 1979;44:127–137.

2. Phelps ME, Huang S-C, Hoffman EJ, Selin C, Sokoloff L, Kuhl DE. Tomographic measurement of local cerebral glucose metabolic rate in humans with (F-18)-2-fluoro-2-deoxy-D-glucose: validation of method. Ann Neurol 1979;6:371–388.

3. Huang S-C, Phelps ME, Hoffman EJ, Sideris K, Selin CJ, Kuhl DE. Noninvasive determination of local cerebral metabolic rate of glucose in man. Am J Physiol 1980;238:E69–E82.

4. Sokoloff L, Reivich M, Kennedy C, et al. The (^{14}C)-deoxyglucose method for the measurement of local cerebral glucose utilization: theory, procedure and normal values in the conscious and anesthetized albino rat. J Neurochem 1977;28:897–916.

5. Phelps ME, Mazziotta JC, Schelbert HR. Positron emission tomography and autoradiography. Principles and applications for the brain and heart. New York: Raven Press; 1986.

6. Hawkins RA, Hoh C, Dahlbom M, et al. PET cancer evaluations with FDG. J Nucl Med 1991;32:1555–1558.

7. Haberkorn U, Strauss LG, Dimitrakopoulou A, et al. PET studies of fluorodeoxyglucose metabolism in patients with recurrent colorectal tumors receiving radiotherapy. J Nucl Med 1991;32:1485–1490.

8. Kubota K, Ishiwata K, Kubota R, et al. Tracer feasibility for monitoring tumor radiotherapy: a quadruple tracer study with fluorine-18-fluorodeoxyglucose or fluorine-18-fluorodeoxyuridine,L-[methyl-^{14}C]methionine, [6-^{3}H]thymidine, and gallium-67. J Nucl Med 1991;32:2118–2123.

9. Minn H, Paul R, Ahonen A. Evaluation of treatment response to radiotherapy in head and neck cancer with fluorine-18-fluorodeoxyglucose. J Nucl Med 1988;29:1521–1525.

10. Abe Y, Matsuzawa T, Fujiwara T, et al. Clinical assessment of therapeutic effects on cancer using ^{18}F-2-fluoro-2-deoxy-D-glucose and positron emission tomography: preliminary study of lung cancer. Int J Radiat Oncol Biol Phys 1990;19:1005–1010.

11. Nagata T, Yamamoto K, Hiraoka M, et al. Monitoring liver tumor therapy with [^{18}F]FDG positron emission tomography. J Comput Assist Tomogr 1990;14:370–374.

12. Wahl RL, Cody R, Zasadny K, et al. Active breast cancer chemohormonotherapy sequentially assessed by FDG PET: early metabolic decrements precede tumor shrinkage [Abstract]. J Nucl Med 1991;32:982.

13. Hawkins RA, Phelps ME, Huang SC. Effects of temporal sampling, glucose metabolic rates and disruptions of the blood-brain barrier (BBB) on the FDG model with and without a vascular compartment: studies in human brain tumors with PET. J Cereb Blood Flow Metab 1986;6:170–183.

14. Di Chiro G. Positron emission tomography using [^{18}F]fluorodeoxyglucose in brain tumors. Invest Radiol 1987;22:360–371.

15. Adler LP, Blair HF, Makley JT. Noninvasive grading of musculoskeletal tumors using PET. J Nucl Med 1991;32:1508–1512.

16. Horton RW, Meldrum BS, Bachelard HS. Enzymic and cerebral metabolic effects of 2-deoxy-D-glucose. J Neurochem 1973;21:506–520.

17. Som P, Atkins HL, Bandoypadhyay D, et al. A fluorinated glucose analog, 2-fluoro-2-deoxy-D-glucose (^{18}F): nontoxic tracer for rapid tumor detection. J Nucl Med 1980;21:670–675.

18. Warburg O. The metabolism of tumors. London: Constable & Co.; 1930.

19. Warburg O. On the origin of cancer cells. Science 1956;123:309–314.

20. Flier JS, Mueckler MM, Usher P, Lodish HF. Elevated levels of glucose transport and transporter messenger RNA are induced bas ras or src oncogenes. Science 1987;235:1492–1495.

21. Okazumi S, Isono K, Enomoto K, et al. Evaluation of liver tumors using ^{18}F-fluorodeoxyglucose PET: characterization of tumor and assessment of effect of treatment. J Nucl Med 1992;33:333–339.

22. Hoffman EJ, Phelps ME. Positron emission tomography: principles and quantitation. In: Phelps ME, Mazziotta JC, Schelbert HR, eds. Positron emission tomography and autoradiography. Principles and applications for the brain and heart. New York: Raven Press; 1986:237–286.

23. Guerrero TM, Hoffman EJ, Dahlbom M, et al. Characterization of a whole body imaging technique for PET. IEEE Trans Nucl Sci 1990;37:676–680.

24. Tse N, Hoh CK, Hawkins RA, et al. Application of positron emission tomography with 2-[F-18]fluoro-2-deoxy-D-glucose (FDG) to the evaluation of breast masses. Ann Surg 1992: in press.

25. Yu DC, Huang SC, Grafton ST, et al. Methods for improving quantitation of putamen uptake constant of FDOPA in PET studies. J Nucl Med 1992:submitted.

26. Germano G, Chen BC, Huang SC, et al. Use of the abdominal aorta for arterial input function determination in hepatic and renal PET studies. J Nucl Med 1992:in press.

27. Gambhir SS. Quantification of the physical factors affecting the tracer kinetic modeling of cardiac positron emission tomography data [PhD dissertation]. University of California, Los Angeles, 1990.

28. Huang SC, Phelps MR, Hoffman EJ, Kuhl DE. Error sensitivity of fluorodeoxyglucose method for measurement of cerebral metabolic rate of glucose. J Cereb Blood Flow Metab 1981;1:391–401.

29. Baron JC, Frackowiak RSJ, Herholz K, et al. Use of PET methods for measurement of cerebral energy metabolism and hemodynamics in cerebrovascular disease. J Cereb Blood Flow Metab 1989;9:723–742.

30. Huang SC, Mahoney DK, Phelps ME. Quantification in positron emission tomography. 8. Effects of nonlinear parameter estimation on functional images. J Comput Assist Tomogr 1987;11:314–325.

31. Schmidt K, Mies G, Sokoloff L. Model of kinetic behavior of deoxyglucose in heterogeneous tissues in brain: a reinterpretation of the significance of parameters fitted to homogeneous tissue models. J Cereb Blood Flow Metab 1991;11:10–24.

32. Herholz K, Patlak CS. The influence of tissue heterogeneity on results of fitting nonlinear model equations to regional tracer uptake curves: with an application to compartmental models used in positron emission tomography. J Cereb Blood Flow Metab 1987;7:214–229.

33. Hawkins RA. Radionuclide studies of the liver and hepatobiliary system. Current Opinion in Radiology 1989;1:499–507.

34. Bassingthwaighte JB. A concurrent flow model

for extraction during transcapillary passage. *Circ Res* 1974;35:483–503.

35. Choi Y, Hawkins RA, Huang SC, et al. Parametric images of myocardial metabolic rate of glucose generated from dynamic cardiac PET and 2-[¹⁸F]fluoro-2-deoxy-d-glucose studies. *J Nucl Med* 1991;32:733–738.

36. Weinberg IN, Huang SC, Hoffman EJ, et al. Validation of PET-acquired input functions for

cardiac studies. *J Nucl Med* 1988;29:241–247.

37. Patlak CS, Blasberg RG, Fenstermacher JD. Graphical evaluation of blood-to-brain transfer constants from multiple-time uptake data. *J Cereb Blood Flow Metab* 1983;3:1–7.

38. Patlak CS, Blasberg RG, Fenstermacher J. Graphical evaluation of blood-to-brain transfer constants from multiple-time uptake data. Generalizations. *J Cereb Blood Flow Metab*

1985;5:584–590.

39. Messa C, Choi Y, Hoh CK, et al. Quantitative analysis of FDG uptake in metastatic melanoma: utility of parametric imaging with PET [Abstract]. *J Nucl Med* 1991;32:1838.

40. Herholz N. Non-stationary spatial filtering and accelerated curve fitting for parametric imaging with dynamic PET. *Eur J Nucl Med* 1988;14:477–484.

SELF-STUDY TEST
Radiobiology and Radiation Protection
ANSWERS

ITEMS 1-5: Effects of Acute Whole-Body Radiation Exposure
ANSWERS: 1, T; 2, F; 3, T; 4, F; 5, F
In general, whole-body doses over 100 rads have significant effects on immune system responsiveness. A whole-body exposure of 100 rads will reduce the peripheral blood lymphocyte count by about 50%. In fact, the immunosuppressive properties of whole-body radiation have been used to prevent rejection of transplanted organs.

The dose in humans that produces permanent sterilization is about 500–600 rads. Such an effect is highly unlikely from a whole-body radiation exposure because a dose of this magnitude is likely to be lethal before sterility is manifest. In males, doses as low as 15–30 rads markedly reduce the sperm count at about 8 wk after exposure. The sperm count slowly recovers over the next several months. At doses above 100–150 rads, the sperm count begins to fall earlier, and after falling practically to zero may recover, but very slowly.

Even with high doses of radiation the likelihood of radiation-induced cancer in an irradiated individual is small. For a whole-body dose of 100 rads the lifetime risk of radiation-induced fatal cancer is about 1%. The risk of radiation-induced genetic effects in the offspring of such irradiated individuals would be quite small. In fact, the study of 18,946 children born to parents who were A-bomb survivors (with a mean dose of 117 rads received jointly by the two parents) showed no statistically significant increase in stillbirths, congenital defects, premature death, and abnormal blood proteins.

Epilation and bleeding of gums would be quite unlikely after a dose of 100 rads; these effects generally occur after doses of about 400 rads.

ITEMS 6-10: Nonstochastic Effects
ANSWERS: 6, T; 7, F; 8, T; 9, T; 10, F
Nonstochastic effects of radiation are those for which the severity, rather than the probability, of an effect varies with the dose, and for which a threshold may occur. Nonstochastic effects of radiation include nonmalignant damage to the skin, cell depletion of the bone marrow, induction of cataracts, and gonadal cell damage leading to impaired fertility. Because the thresholds for these effects are well above the dose equivalent limits for occupational exposure, these nonstochastic effects can be prevented.

Stochastic effects (carcinogenesis) appear to saturate at high doses—the likely explanation for this phenomenon is cell killing. Many nonstochastic effects, on the other hand, specifically occur as a result of cell killing.

ITEMS 11-14: Genetically Significant Dose
ANSWERS: 11, F; 12, F; 13, F; 14, T
The genetically significant dose (GSD) is *not* the dose of radiation each person receives from birth to death and is *not* the dose of radiation that can be shown to lead to a genetic death. Rather, the GSD is an index of the presumed genetic impact of radiation exposure on the population. The GSD is defined as the dose that, if received by every member of the population, would be expected to produce the same total genetic injury to the population as is produced by the actual doses received by various individuals. The GSD for medical radiations is calculated from the frequency of the particular examination in a certain age group of the population, the corresponding gonadal doses and the appropriate weighting factors that take into account the expectancy of offspring in the population. Because the presumed genetic injury is *only* associated with the offspring of irradiated individuals, estimation of GSD from the

gonadal doses received by these individuals requires that these doses be weighted for the probability of offspring, i.e., not only must there be gonadal radiation, there must be a probability of offspring for it to have a genetic effect. A nuclear medicine procedure resulting in gonadal radiation exposure to a 70-yr-old woman would not contribute to the GSD because the probability of offspring is nil. The annual contributions to the GSD from background, diagnostic radiology, and nuclear medicine procedures in the U.S. are: 82, 20, and 2–4 mrems/year, respectively.

Reference
1. Mettler FA, Williams AG, Apar JA, Kelsey CA. Estimation of the genetically significant dose from nuclear medicine examinations in the United States: 1980. *Health Phys* 1986;51:377–379.

ITEMS 15-19: Genetic "Doubling Dose"
ANSWERS: 15, T; 16, F; 17, F; 18, T; 19, F
By definition, the doubling dose is the amount of radiation that would be expected to add as many new mutations as occur spontaneously. Thus, the higher the doubling dose, the lower would be the risk of mutation from any particular radiation dose. The doubling dose is the reciprocal of the relative mutation risk, the fraction by which each added rad of radiation dose would increase the mutation rate above the spontaneous level. Thus, a relative mutation rate of 0.01/rad, a risk of 1/100 per rad, would give a doubling dose of 100 rads. A doubling dose would not double the incidence of mutations in the next generation but would require several generations to be fully expressed, i.e., to reach a new equilibrium. This is because elevations in radiation dose must persist over many generations to result in a new and higher mutation burden in the gene pool of the population. Mutant genes are eliminated from the population faster as the number of mutant genes in the population increases. Eventually (after perhaps ten or more generations) a balance will occur between the rate of increase and elimination of mutations and a new "equilibrium" will be established.

The BEIR-1980 estimate of a doubling dose of 50–250 rads was obtained from data on mice because no genetic effects have been observed in humans.

References
1. Searle AG. Hereditary damage. *Radiat Environ Biophys* 1979;17:41–46.
2. Selby PB. Genetic effects of low-level irradiation. In: Fullerton GD, Kopp DT, Waggener RG, Webster EW, eds. *Biological Risks of Medical Irradiation.* Medical Physics Monograph No. 5. New York: American Institute of Physics, 1980:1–20.

ITEMS 20-24: Genetic Effects of Radiation
ANSWERS: 20, T; 21, F; 22, F; 23, F; 24, T
Mutations are almost always detrimental to the organism. Any gene, presumably, is the bearer of some bit of valuable genetic information, a particular command that must be executed if the cell is to function properly. In its mutated form the gene's "action" will be missing.

Because there is no direct evidence in humans of radiation-induced genetic damage (even in the progeny of the A-bomb survivors) it has been necessary to rely on animal studies to estimate the risk to humans. Animal studies have revealed that the type and magnitude of the genetic effect depends on: (1) the stage of germ cell development at irradiation (immature germ cells appear to be capable of repair, whereas, in mature germ cells there is little or no repair); (2) dose rate (lower dose rates and fractionation produce fewer mutations); and (3) the interval between